

## EXPERIMENTAL INVESTIGATION OF THE CONVECTIVE CONDENSATION HEAT TRANSFER IN MICROCHANNEL FLOWS

**Roger R. Riehl**

Mechanical Engineering Department – Federal University of Santa Catarina, Florianopolis, SC 88040-900 Brazil  
rriehl@cet.ufsc.br

**Jay M. Ochterbeck**

Department of Mechanical Engineering – Clemson University, Clemson, SC 29634 USA  
jochter@ces.clemson.edu

***Abstract.** This paper presents experimental results toward the improvement of condensation capabilities for miniature systems with restricted heat dissipation area. Two pumping systems were used in an experimental apparatus to test microchannel condensers with methanol as the working fluid. Tests were conducted for two different saturation temperatures, for a range of heat dissipation rate from 20 to 350 W and four microchannel condensers. The results showed that the condensers presented high heat transfer capabilities with Nusselt numbers on a range of 15 to 600, despite the small heat transfer areas (0.0018-0.00105 m<sup>2</sup>). A Nusselt number correlation was obtained and shown to correlate 95% of the data within an error range of less than 25%.*

***Keywords.** Convective condensation, microchannel, thermal control, heat transfer.*

### 1. Introduction

With the miniaturization of electronic devices and systems, area restrictions for the heat to be dissipated can become a significant problem. This issue became important when considering that the device performance and reliability are known to increase when operating temperatures are kept below 80 °C. In space applications, capillary pumped loops (CPL) and loop heat pipes (LHP) have been used as thermal management devices for electronics and structures, being able to transport heat from a high temperature source to a low temperature sink with minimal temperature difference. Due to restricted areas on satellites, new designs of condensers have to be conceived.

With such conditions, many investigations were performed during the last two decades towards electronics device cooling. Investigations and applications using forced-air convection were the first attempts for electronic device heat dissipation. Air-cooled systems are currently still used, but correspond to limited heat transfer capabilities. For the continuing increases in heat flux, microchannel convective flows have been addressed to overcome some issues related to forced-air convection and pool boiling systems. Tuckerman and Pease (1981) first proposed a cooling system for electronic devices using microchannel flows for forced single-phase liquid. This technology demonstrated promise for more compact arrangements of electronic devices and cooling systems in future electronic packaging. Based upon initial findings, a compact heat-sink microchannel was found to offer new degrees of freedom for system designs with considerable higher cooling rates, but very significant high-pressure penalty.

Many investigations were performed using microchannel flows, using single and two-phase convective flow. A literature survey of single-phase and two-phase flow heat transfer coefficients was presented by Riehl et al. (1998) and reviewed the available analytical models and experimental data obtained for microchannels. The results obtained, when compared to each other, showed a wide dispersion. From the available information, the so-called general correlations are not able to predict the heat transfer coefficient for microchannel application. Other correlations developed for microchannel convective flow, present great dispersions when compared to each other for the same operation conditions. One of the few works reported regarding condensation in microchannel was presented by Begg et al. (1999). In this work, a thermosyphon was used to test several individual microchannel tubes, where an analysis was performed by flow visualization of the condensing section. They concluded that the condensation film in such channels is very restricted due to surface tension effects.

In the current investigation, four different microchannel heat exchangers were experimentally tested for condensing two-phase flow in order to determine the Nusselt number and to aid development of a correlation. An experimental apparatus was designed and built to test the microchannel condensers in order to verify behavior of the heat transfer at low and high flow rates. This procedure has the objective of helping future microchannel heat exchanger design, and to improve electronics and capillary pumped cooling systems.

## 2. Experimental apparatus

To test the microchannel condensers, two pumping methods were used: the first was a capillary evaporator and the second was a magnetic driven pump in conjunction with a flow through evaporator. The capillary evaporator was used for testing at low flow rates along the condensation section, while the mechanic pump promoted higher flow rates. The condensers were designed considering that, as the channel size decreased the number of parallel channels increased. This design was important in tests using the capillary evaporator (CPL mode), since this system presents limitations regarding the maximum allowed pressure drop. Such systems present some limitations regarding its pumping capacity, as the entire flow is driven by capillary forces. The capillary evaporator presented several other advantages as a pumping device, such as the flowrate is controlled by the heat load applied on the evaporator.

For the tests when higher flow rates had to be reached, a leak-free magnetic driven pump with speed control was used. This pump allowed controlling the flow rate up to a maximum of 3 l/min for a maximum pressure drop of 275 kPa. The details on the design for the loop configuration used for testing the microchannel condensers are presented by Riehl (2000).

### 2.1. Experimental apparatus with a capillary pumped loop (CPL) evaporator

The use of a CPL presented several advantages for testing the microchannel condensers. Stenger (1966) at the NASA Lewis Research Center first proposed the capillary pumped loop (CPL), which is a two-phase thermal management system. Basically the CPL uses capillary forces to pump a working fluid from a heat source to a heat sink. This system is able to transfer heat efficiently with a small temperature differential and no external power requirements (Faghri, 1995). Heat is acquired in a capillary evaporator and rejected using a condenser. The system is passively pumped by means of surface tension forces developed in a porous structure (called a wick) located in the evaporator (Ku, 1997). Major advantages of a CPL include no moving parts and high heat transport capabilities. Disadvantages include that a CPL requires sub cooling and the maximum pressure is limited. In the proposed CPL apparatus, a by-pass condenser was used to better control the vapor volume in the microchannel condenser. Both by-pass condenser and sub-cooler were tube-in-tube heat exchangers. On the test section, heat was removed from the microchannel condenser by a cold plate, placed at the condenser base, which used a mixture 50 % ethylene glycol and 50 % water as working fluid and a rotameter was used to measure the flowrate. Figure 1 presents the experimental apparatus used for testing the microchannel condensers on the CPL mode and the instrumentation used (discussed later). This apparatus was built with stainless steel tubes with outer diameter of 6.35 mm for both liquid and vapor lines. The vapor line had a total length of 1.0 m and the liquid line 1.8 m.

### 2.2. Experimental apparatus with a magnetic driven pump

The objective of using a magnetic driven pump was to reach higher flow rates and, consequently, higher pressure drops along the condensation section to better analyze the heat transfer capability of such. Figure 2 shows the experimental apparatus with the magnetic driven pump. The magnetic driven pump was equipped with a DC motor and a variable speed control. A flowmeter was added to the apparatus to measure the liquid flow rate, which was displayed on a LCD and the signal was also taken by the data acquisition system. All other parts of the experiment were identical to those described in Section 2.1.

### 2.3. Instrumentation and Data Acquisition

Twenty-one type-T thermocouples were used, along with two pressure transducers (one absolute and one differential). Thermocouples 20 and 21 were placed at each side of the condenser, in order to obtain the wall temperature. Thermocouples 01 and 02 measured the inlet and outlet temperatures of the ethylene glycol, respectively.

An absolute pressure transducer was used to measure the working fluid operation pressure, which was set using a two-phase reservoir. A differential pressure transducer was used to measure the pressure drop along the condensation section. The pressure transducers were manufactured and calibrated by Sensotec Inc. For the absolute and differential pressure transducers, the output signal was 2 mV/V for a maximum excitation of 10 VDC. A description of the instruments used and uncertainties is presented on Table 1.

All instruments listed above were connected to a data acquisition system, manufactured by National Instruments. This system was composed of a data acquisition card type AT-MIO-16XE-50, a chassis type SCXI-1000, a module type SCXI-1100 and a terminal block type SCXI-1303. This system was controlled by a Pentium-MMX 166 MHz computer. The signals from the instruments were taken under a gain of 100, at a rate of 1 reading per second and filtered at 0.5 Hz. To monitor, control and acquire the results, a G-program was written using LabVIEW software version 5.1. The results were saved in a spreadsheet data file, where the data reduction could be performed.

Table 1. System instrumentation.

Instrument	Type/Model	Manufacturer	Accuracy	Reading Scale
Thermocouple	type-T	Omega	$\pm 0.3 \text{ }^\circ\text{C}$	-100 to 300 $^\circ\text{C}$
Rotameter	C7646	Omega	$\pm 2.0 \%$	0 to 100 ml/min
Absolute Pressure Transducer	THE/0713 – 04TJA	Sensotec	$\pm 0.5 \%$	0 to 344.5 kPa
Differential Pressure Transducer	A5/882 – 22A5 – D	Sensotec	$\pm 0.25 \%$	0 to 172.25 kPa
Digital Multimeter	34401A	Hewlett Packard	$\pm 0.0045 \%$	0 to 100 V
Flowmeter	112	McMillian	$\pm 1 \%$	0 to 5 l/min

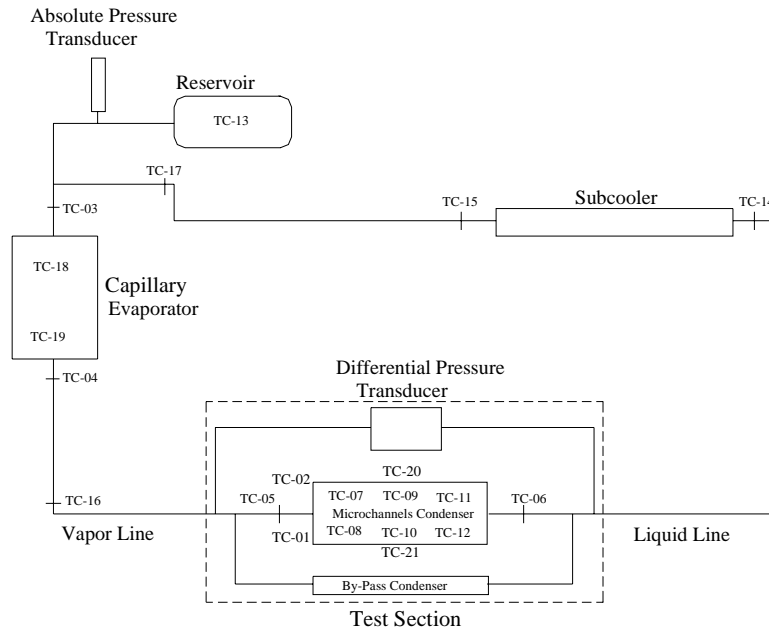


Figure 1. Experimental apparatus using CPL mode.

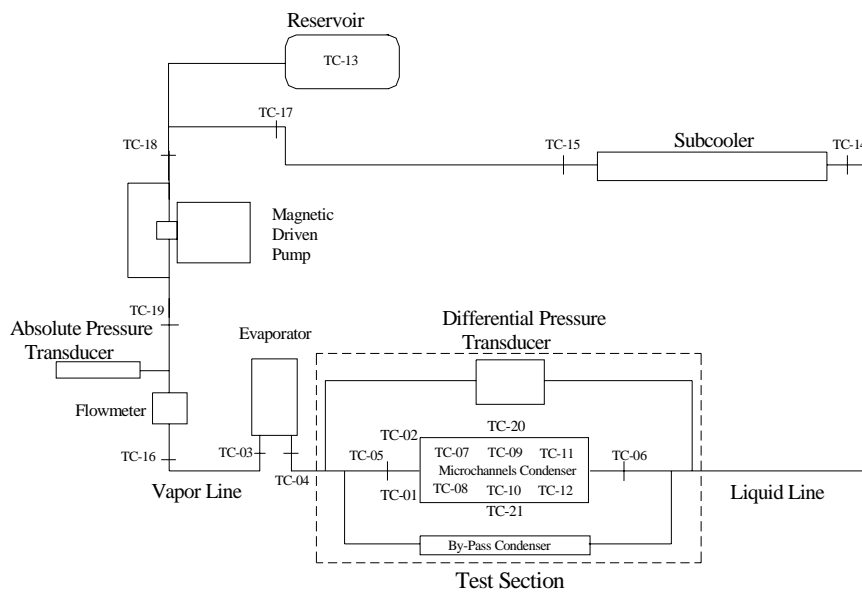


Figure 2. Experimental apparatus with a magnetic driven pump.

## 2.4. Experimental procedure

Tests were performed over a total condensation length of 150 mm and were conducted with the same procedure for all condensers when either the capillary evaporator or the magnetic pump was used. The tests for the condensers were performed following the procedure as shown on Table 2. Independent of the pump used to perform the tests, each condenser was tested under two different saturation temperatures and different levels of heat load applied to the evaporator. For the tests with the capillary evaporator, the range of flow rate was dependent on the heat load applied to the evaporator. For the tests where a mechanic pump was used, the range of flow rate varied for each condenser, which was dependent on the presence of two-phase flow in the channels. Table 3 shows the characteristics of all condensers.

Table 2 – Test procedure for the condensers.

Apparatus	Working Fluid	Operation Temperatures	Heat Input to the Evaporator	Acquisition Time During Steady State
Capillary Evaporator	Methanol	45 and 55 °C	20 to 120 W	1000 sec
Magnetic Pump	Methanol	45 and 55 °C	175 to 350 W	1000 sec

Table 3. Characteristic of the microchannel condensers.

Condenser	Channel Dimensions (mm)	Aspect Ratio	Number of Channels	Total Heat Transfer Area(m <sup>2</sup> )
1	1.50	1.0	8	0.00180
2	1.00	1.0	10	0.00150
3	0.75	1.0	12	0.00135
4	0.50	1.0	14	0.00105

All microchannel condensers tested used a poly-carbon cover to allow flow visualization, which was performed by a digital Panasonic DCC camera with 32 frames/sec. The flow visualization was used to verify the two-phase flow distribution in the channels.

After the installation of each microchannel condenser, several steps were followed to ensure reliability of the results. First, the loop had to hold and be under vacuum of  $10^{-3}$  mTorr ( $1.33 \times 10^{-7}$  kPa) for 24 hours. This procedure had to be taken to ensure the absence of non-condensable gases (NCG) in the loop. Then, an amount of methanol was used to charge the loop. The absence of NCG was verified by comparing the absolute pressure (taken from the direct reading of the absolute pressure transducer) with the vapor pressure at the reservoir temperature.

After charging, the reservoir temperature was raised to the desired operational temperature, using a silicon heater attached to its wall, where a thermostat was used to control the temperature range. After reaching the operating temperature, the system was ready to start operating.

For the tests where the capillary evaporator was used, heat was applied to the system through the capillary evaporator over a range of 20 to 120 W. For this range, just laminar flow for both liquid and vapor phases was verified. Heat was applied to the capillary evaporator by a silicon heater placed at the evaporator's vapor container wall. The heat applied was controlled by a Variac, connected to a digital multimeter. The tests were performed until steady state was reached for the given heat load applied to the capillary evaporator. The by-pass condenser was designed to be used if more condensation capability was required, when starting the capillary evaporator. However, the by-pass condenser was not needed during the tests.

For the tests where the magnetic pump was used, heat was applied to the evaporator through the silicon heater attached to its upper surface while the pump was started at a low flow rate of working fluid. When steady state was reached for a given flow rate and applied power, the flow rate was then increased to the next level. If, for a certain flow rate, no more two-phase flow was verified, higher power was applied to the evaporator and the tests were started again for a low flow rate of working fluid.

The objective of the tests was to acquire temperature and pressure (differential) readings throughout the loop. The temperature readings were used to obtain the heat transfer coefficient, converted later to the Nusselt number. The differential pressure readings were used to verify the pressure drop across the condensation section during the tests.

## 2.5. Data Analysis

The results related to the Nusselt number and pressure drop were obtained from the readings of 21 thermocouples and two pressure transducers, installed in the apparatus. As the heat load could be calculated by the relation

$$\dot{Q} = \frac{V^2}{R} \quad (1)$$

where  $V$  is the voltage (V) and  $R$  the resistance (Ohms), the mass flow rate could be calculated (when using the capillary evaporator) by the equation:

$$\dot{m} = \frac{\dot{Q}}{i_v}, \quad (2)$$

where  $\dot{m}$  is the mass flow rate (kg/s) and the saturation temperature ( $T_{sat}$ , °C) was used to evaluate the latent heat of vaporization ( $i_v$ , J/kg), related to the heat transfer rate ( $\dot{Q}$ , in W). For the case when a mechanic pump was used, the flow rate was obtained directly from the flowmeter.

The temperatures obtained from the thermocouples on the condensing section were then used to calculate the heat transfer coefficient ( $h$ , W/m<sup>2</sup>°C). Thus, the rejected heat ( $\dot{Q}_R$ ) could be obtained from the equation:

$$\dot{Q}_R = \dot{m}_{cool} c_{p,cool} (T_o - T_i), \quad (3)$$

where  $\dot{m}_{cool}$  is the cooling fluid flow rate (kg/s) measured using a rotameter,  $c_{p,cool}$  is the cooling fluid specific heat (J/kg °C) and  $T_o$  and  $T_i$  are the outlet and inlet cooling fluid temperature respectively. The mean heat transfer coefficient ( $\bar{h}$ ) was then calculated using the Newton's Law of Cooling as

$$\bar{h} = \frac{\dot{Q}_R}{A(T_{sat} - T_w)}. \quad (4)$$

where  $A$  is the heat transfer area (m<sup>2</sup>) and  $T_w$  is the wall temperature (°C). Finally, the Nusselt number was calculated using the following equation

$$Nu = \frac{\bar{h} D_h}{k_l}, \quad (5)$$

where  $k_l$  is the liquid thermal conductivity (W/m °C). For each power level applied to the evaporator, the Nusselt number was evaluated to later obtain the behavior of each parameter with the heat rejected. The pressure drop data was obtained directly by the differential pressure transducer, where a mean value of the results was performed for each test. The results for Nusselt number were then used to obtain a correlation.

The uncertainties on the experimental results were performed according to Moffat (1985). For tests regarding heat transfer, Moffat (1985) suggests that the uncertainty analysis must be performed by single-sample method. The equation to evaluate the total uncertainty on the heat transfer coefficient results becomes:

$$\delta \bar{h} = \left\{ \left[ \left( \frac{1}{A(T_{sat} - T_w)} \right) \delta \dot{Q}_R \right]^2 + \left[ \left( -\frac{\dot{Q}_R}{A(T_{sat} - T_w)^2} \right) \delta T \right]^2 + \left[ \left( \frac{\dot{Q}_R}{A(T_{sat} - T_w)^2} \right) \delta T \right]^2 \right\}^{\frac{1}{2}}. \quad (6)$$

Considering the reading deviations of all instruments and applying them on the above uncertainty analysis, the overall uncertainties on the experimental results were varying from 5 to 10 %.

## 2.6. Data Reduction

A data reduction program was done, using the software MathCAD 8.0. The input data were the temperatures, absolute and differential pressures, the working fluid flow rate (when using the capillary evaporator, the input was the heat applied to it), the cooling fluid flow rate verified during the experimental tests and the geometric parameters of the transport lines and condenser.

A two-phase pressure drop model was applied for this data reduction program, based on the Separated Flow Model (Collier, 1981). The pressure drop model then calculated the two-phase length in the condenser, and an interactive method was used to perform all the calculations, where the final results were the Nusselt Number and pressure drop, with the respective uncertainties.

## 3. Experimental results

The experimental results obtained with both pumps (CPL and magnetic pump) were separately analyzed. This procedure had to be performed in order to evaluate the heat transfer capabilities of all microchannel condensers at different working conditions, i.e., according to the vapor quality at the condensation section inlet.

Due to the CPL working conditions, only vapor with a slight superheat leaves the capillary evaporator. Thus, at the microchannel condenser inlet, essentially saturated vapor was present. In the case of a magnetic pump driving the fluid throughout the loop, the vapor quality at the microchannel condenser inlet varied for each condition. As the heat load to the evaporator and liquid flow rate varied, the vapor quality at the condenser inlet also varied on a range from 10 to 55%.

### 3.1. Results for tests using the capillary evaporator

The heat transfer coefficients calculated per channel, using Newton’s Law of Cooling, were compared for all microchannel condensers tested. The Nusselt number increased with the heat load applied to the evaporator (which increased the flow rate) and rejected by the condenser, on a linear pattern.

When comparing the results for both operation temperatures, it could be observed that the Nusselt number for  $T_{sat}=45\text{ }^{\circ}\text{C}$  is higher than that for  $T_{sat}=55\text{ }^{\circ}\text{C}$ . Figure 3 presents the Nusselt number versus the liquid Reynolds number obtained per channel, at both operation temperatures. It is interesting to note that even using different heat transfer areas, the Nusselt number did not show a wide dispersion.

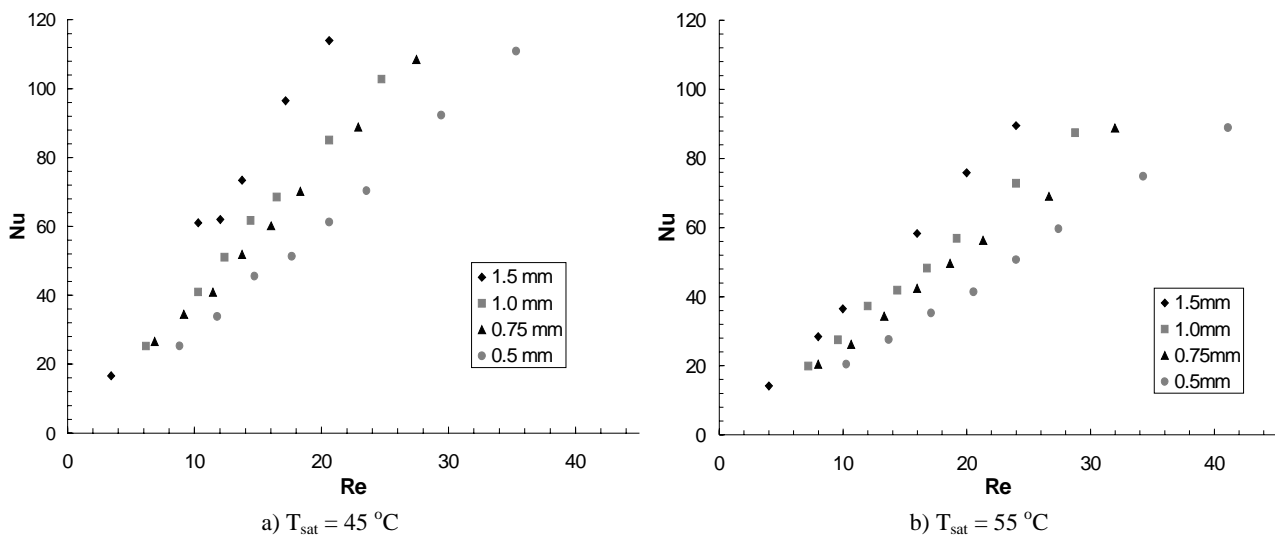


Figure 3 – Nusselt number versus liquid Reynolds number for both saturation temperatures.

Just the condenser with channels of 0.5 mm presented greater temperature differences, which resulted in higher Nusselt number when compared to the other condensers. Such characteristic was observed for all the tests, which showed that the condenser with channel size of 0.5 mm could present greater heat transfer capabilities, influenced by the geometric parameters

On the same way, the fact that only laminar liquid flow was verified in the channels, it emphasized the great heat transfer capability that such microchannel condensers could present. A special attention should be given to the pressure drop along the condensers, as higher pumping power would be required.

### 3.2. Results for tests using the magnetic pump

The magnetic pump presented an operation slightly different than with the capillary evaporator, but the overall operation characteristics during the tests were basically the same. As the magnetic pump promoted higher flow rates than those observed with the capillary evaporator. As the capillary evaporator, the magnetic pump allowed controlling the flow rate, which was kept constant during the tests. The range of flow rate applied to each test varied depending on the power input to the evaporator, which was dependent on the presence of two-phase flow. For higher power, wide ranges of flow rate could be obtained, which allowed the observation of different flow conditions in the condensers.

As well as for the tests using the capillary evaporator, the tests using the magnetic pump presented high values for the Nusselt number. Although higher values of Nusselt number were expected due to the higher flow rate, the presented results showed that the Nusselt number for the condensers tested depends also on the flow pattern observed during the tests (Riehl, 2000). Figure 4 presents the Nusselt number for the saturation temperatures of 45 and 55 °C, respectively.

As observed in the previous results, the Nusselt number increased with the increasing flow rates for both saturation temperatures. Higher Nusselt numbers were achieved for higher flow rates of liquid for both saturation temperatures, while the vapor flow rate (controlled by the heat load applied to the evaporator) was kept constant, also resulting in different flow conditions observed during the tests. For low flow rates (as those achieved using the capillary evaporator), laminar flow for both liquid and vapor phases were observed. For higher flow rates, in some cases, laminar flow for both liquid and vapor phases were also observed. For other cases (higher heat input to the evaporator) the vapor phase presented a behavior similar to turbulent flow and the liquid phase presented in the limit to the transition

from laminar to turbulent, when compared to greater channel diameters. Such behavior was more clearly observed when analyzing the absolute pressure of the loop and the pressure drop along the condenser. The absolute pressure presented great variations when the flow was close to the transition and the pressure drop measurement were very unstable. A detailed analysis the phenomenon is presented by Riehl (2000).

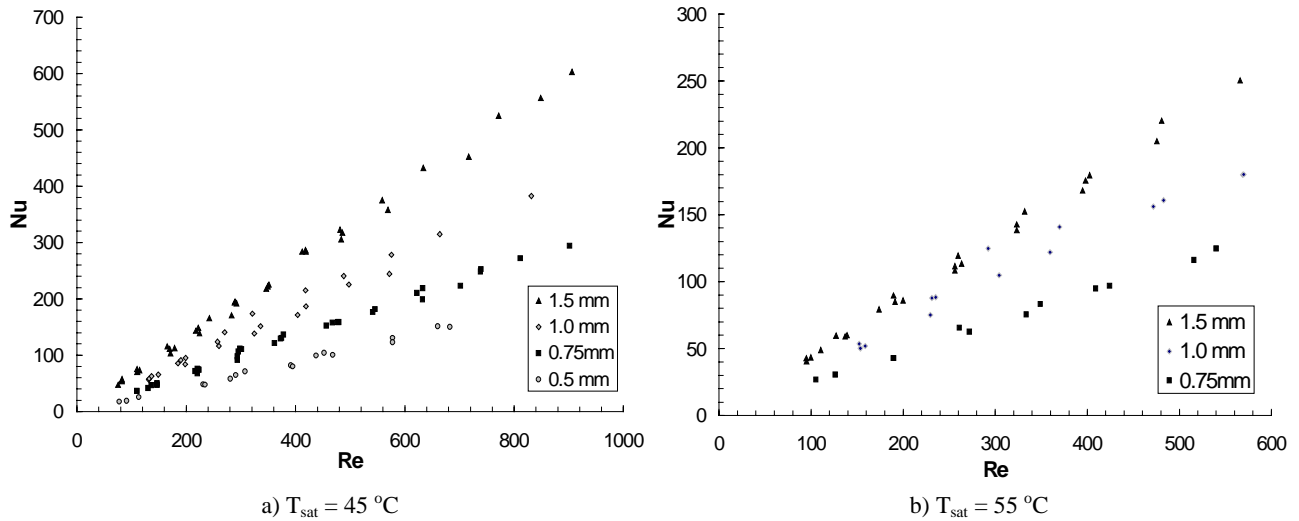


Figure 4 – Nusselt number versus liquid Reynolds number for tests using a magnetic pump.

### 3.3. Nusselt number correlation

With the experimental results for the Nusselt number for both ranges of flow rate tested, it was necessary to obtain an equation that correlates the results. A review of the literature regarding existing correlations for Nusselt number, showed great dispersion on the results (Riehl et al., 1998). Thus, an empirical equation was obtained to calculate the Nusselt number based on the form:

$$Nu = We^{-Ja} Re_{Dh} Pr^Y, \quad (6)$$

where dimensionless parameters  $We$ ,  $Ja$ ,  $Re_{Dh}$ , and  $Pr$  are the Weber, Jacob, Reynolds and Prandtl numbers respectively. The liquid Reynolds number, based on the hydraulic diameter, is defined as

$$Re_{Dh} = \frac{GD_h}{\mu_l}, \quad (7)$$

where  $G$  is the mass velocity ( $\text{kg/m}^2 \text{ s}$ ),  $D_h$  is the hydraulic diameter (m) and  $\mu_l$  is the dynamic viscosity (Pa.s). The Prandtl and Jacob numbers are defined as:

$$Pr = \frac{\mu_l}{\rho_l c_{pl}}, \quad (8)$$

$$Ja = \frac{c_{pl}(T_w - T_{sat})}{i_{lv}}, \quad (9)$$

where  $\rho_l$  is the liquid density ( $\text{kg/m}^3$ ) and  $c_{pl}$  is the liquid specific heat ( $\text{J/kg } ^\circ\text{C}$ ). The exponents on Eq. (6) that correlated best to the experimental results were empirically found to be:

$$Y = 1.3 \quad \text{if } Re \leq 65, \quad (10)$$

$$Y = \frac{0.5D_h - 1}{2D_h} \quad \text{if } Re > 65, \quad (11)$$

The Weber number is defined as:

$$We = \frac{\rho_l V^2 L}{\sigma}, \quad (12)$$

where  $V$  is the working fluid velocity (m/s),  $L$  is the channel length (m) and  $\sigma$  is the working fluid surface tension (N/m).

Figure 5 presents the comparison between the experimental and calculated results, for both cases of low and high flow rates, using Eq. (6). The experimental results, for  $T_{\text{sat}} = 45 \text{ }^\circ\text{C}$ , presented better correlation for condensers with channel sizes of 1.0, 0.75 and 0.5 mm. A wider dispersion was found for the results of the condenser with channel size of 1.5 mm. Such dispersion was not verified when the results for  $T_{\text{sat}} = 55 \text{ }^\circ\text{C}$  are analyzed. As the saturation temperature increases and the channel sizes decrease, such influence on the calculated results is minimized. Upon performing the design of a microchannel heat exchanger, careful attention should be given to this particular characteristic of Eq. (6) when greater channel size is used, as the proposed correlation presents to be very sensitive to this parameter.

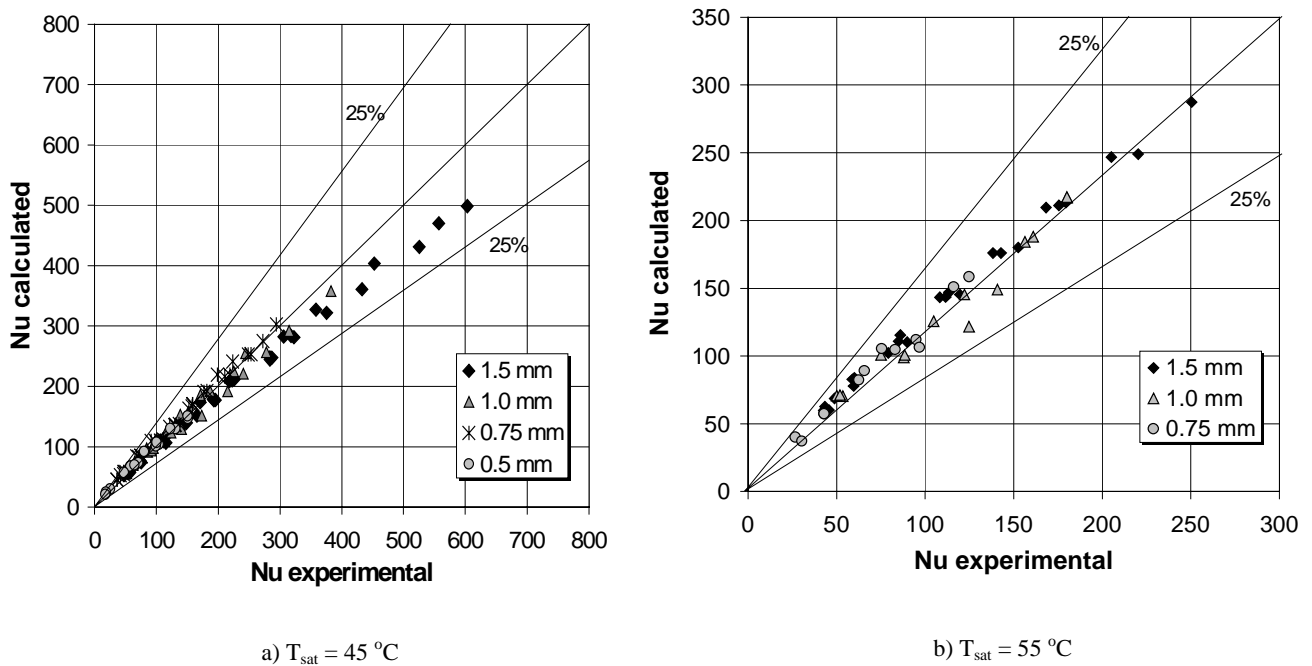


Figure 5 – Comparison of the experimental results and Eq. (6) for both saturation temperatures.

According to the comparison, Eq. (6) correlated 95% of the overall experimental results (for both saturation temperatures and condensers) with a relative error of less than 25%. With such results, Eq. (6) showed a very good correlation capability, which may be used as a tool to design microchannel heat exchangers. The increase on the heat transfer capabilities when applying microchannel condensers in very reduced areas, is specifically important when using it in space radiators where limitation of space, heat dissipation and power consumption are the major concerns in satellite thermal control. The same way, the use of microchannel heat exchangers can lead to a better thermal management of electronics components in several other applications.

#### 4. Conclusions

An experimental investigation regarding convective condensation in microchannels flow was presented. The objective of this study was the investigation of parameters that influence the heat transfer process during condensation in microchannels heat exchangers. The identification of such parameters would be used for microchannel heat exchangers design, applied for micro heat exchangers in order to improve their heat dissipation capabilities. Such experimental investigation was performed to contribute for the knowledge improvement of several variables, present in microchannels flow. Tests were performed for low and high flow rates. For low flow rates, a capillary pumped loop (CPL) was designed and used to test the microchannel condensers where the heat load applied to the capillary evaporator controlled the flow rate. This system presented to be easy to operate and control for all range of heat load applied to the evaporator and saturation temperature. For high flow rates, the capillary evaporator of the CPL was replaced by a magnetic driven pump with flow control, which allowed reaching flow rates that the CPL could not

Tests were performed for four microchannel condensers with different size and number of parallel channels. From the obtained results, it was possible to conclude that the microchannel condensers present high heat transfer rates. High Nusselt numbers were found, proving that it is possible to obtain high heat transfer rates even with reduced areas and



fluid flow rates. This is directly related to geometric factors, which also directly influence the pressure drop. For the case when the magnetic pump was used, higher flow rates, which corresponded to higher Nusselt numbers, could be achieved.

A correlation to predict the Nusselt number was derived. The Nusselt number correlation provided good agreement with the experimental results obtained for all condensers tested. For both saturation temperatures and all condensers tested, 95% of the experimental data was correlated within an error of +/- 25%.

## 5. Acknowledgements

This work was supported by the National Science Foundation through grant CTS-97-30068 (NSF-USA), CAPES (Brasilia-Brazil) and the Fulbright Foundation.

## 6. References

- Begg, E.; Khrustalev, D.; Faghri, A, 1999, "Complete Condensation of Forced Convection Two-Phase Flow in a Miniature Tube", ASME Journal of Heat Transfer, Vol. 121, pp. 904-915.
- Collier, J. G., 1981, "Convective Heat and Mass Transfer". McGraw-Hill International Book Company.
- Faghri, A., 1995, "Heat Pipe Science and Technology", Taylor & Francis.
- Ku, J, 1997, "Recent Advances in Capillary Pumped Loop Technology", National Heat Transfer Conference, Baltimore, MD, August 10-12, pp.1-21.
- Moffat, R. J., 1988, "Describing the Uncertainties in Experimental Results", Experimental Thermal and Fluid Science, Vol. 1, pp. 3-17.
- Riehl, R. R., 2000, "Convective Condensation in Small Diameter Channels With and Without a Porous Boundary", Ph.D. Dissertation, University of São Paulo/Clemson University, 186p.
- Riehl, R. R.; Selegim Jr., P.; Ochterbeck, J. M., 1998, "Comparison of Heat Transfer Correlations for Single- and Two-Phase Microchannel Flows for Microelectronics Cooling", ITherm'98 – Sixth Intersociety Conference on Thermal and Thermomechanical Phenomena in Electronic Systems, Seattle, WA, pp.409-416, May 27-30, 1998.
- Stenger, F. J., 1966, "Experimental Feasibility Study of Water-Filled Capillary Pumped Heat Transfer Loops", NASA TM-X-1310. NASA Lewis Research Center, Cleveland, OH.
- Tuckermann, D. B.; Pease, R. F. W., 1981, "High-Performance Heat Sinking for VLSI", IEEE Electron Device Letters, Vol. EDL-2, No.5, pp. 126-129.